



**Design and Simulation of Non-isolated Bidirectional DC-DC Converter for
Vehicle Application**

Pradeep Kumar Singh

Assistant Professor, Electrical Engineering, Prabhat Engineering College, Kanpur Dehat
pradeepsingh200185@gmail.com

Nitin Kumar

Research Scholar, Electrical Engineering, Prabhat Engineering College
nk8386201@gmail.com

Aman Gupta

Research Scholar, Electrical Engineering, Prabhat Engineering College
amang749902@gmail.com

Nirbhay Singh

Research Scholar, Electrical Engineering, Prabhat Engineering College
nirbhaysingh2563@gmail.com

Abstract-This paper presents the design and simulation of a non-isolated bidirectional DC–DC converter for electric vehicle (EV) applications, focusing on efficient energy transfer between the battery and DC bus. The proposed system integrates a battery energy storage unit with a bidirectional converter that operates in both buck mode (charging) and boost mode (discharging) to support vehicle operation and regenerative energy management. The model is developed and analyzed in MATLAB/Simulink using appropriate control strategies based on pulse width modulation (PWM). The performance of the system is evaluated under different operating conditions, including varying state of charge (SOC) levels, battery charging and discharging characteristics, DC link voltage stability, and load current response. The results demonstrate that the converter ensures smooth and efficient bidirectional power flow, with stable DC link voltage and minimal ripple. The SOC analysis confirms effective charging at lower levels and controlled charging near full capacity, preventing overcharging and enhancing battery life. During discharging, the system provides a consistent and reliable power supply to the load. the proposed non-isolated bidirectional DC–DC converter exhibits high efficiency, reliable operation, and effective energy management, making it suitable for electric vehicle applications, include battery management systems, regenerative braking, and auxiliary power support.

Keywords- Non-isolated Bidirectional DC–DC Converter, Electric Vehicle (EV), Battery Energy Storage System (BESS), State of Charge (SOC), Buck–Boost Converter

I INTRODUCTION

The demand for efficient power conversion systems has been substantially elevated by the rapid expansion of electric vehicles (EVs), hybrid electric vehicles (HEVs), and fuel cell powered vehicles. The bidirectional DC-DC converter is a critical component of these systems, as it is responsible for the efficient management of energy transfer between various power sources

and storage elements. Environmental factors and concerns regarding the depletion of fossil fuels are driving the rapid expansion of electric vehicles (EVs) in the transportation sector worldwide. Different concerns are raised by the swift dissemination of EVs. The most significant obstacle to the proliferation of electric vehicles (EVs) is the development of grid-related power quality issues. Examples of power quality issues that may be induced by the charging process include harmonics, reactive power, voltage reductions and fluctuations, grid frequency instabilities, and unbalanced loads. Simple hardware precautions in the charging block's design can resolve the majority of these issues within the charging station. Nevertheless, the main grid's voltage and frequency instability is a highly intricate and challenging issue to resolve. The primary cause of this issue is the imbalance between energy supply and demand. In this instance, it is not advisable to expand the production-transmission-distribution infrastructure indefinitely. As a result, in recent years, researchers have conducted a plethora of studies on intelligent charging strategies that employ charging topologies such as V2G (vehicle-to-grid), V2H (vehicle-to-home), or V2V (vehicle-to-vehicle) [1,2]. Another area of research for researchers is the practicality of these proposed strategies. Unidirectional energy transfer is implemented in contemporary chargers to facilitate both rapid and gradual charging. Nevertheless, the implementation of these strategies will be unavoidable when the number of electric vehicles (EVs) reaches the present number of conventional vehicles in the future. This is the reason why it is crucial to design slow charging blocks for bidirectional energy transfer. A high-efficiency non-isolated bidirectional DC-DC converter for bidirectional energy transmission is developed in this investigation. The designed bidirectional DC-DC converter has been implemented in both simulation and real-world applications.

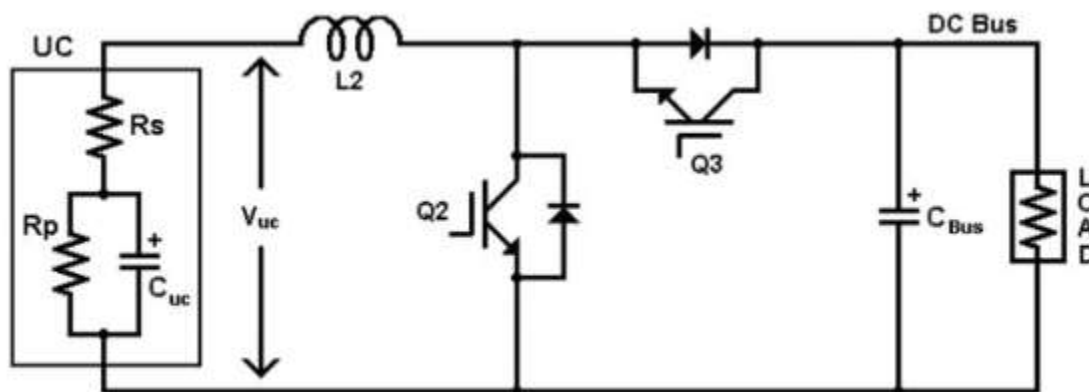


Figure 1. Non-isolated bidirectional DC/DC converter (BC)

The figure depicts a non-isolated bidirectional DC–DC converter that has been integrated with an ultra-capacitor (UC) for the purpose of energy storage and power transfer. The dynamic behaviour of the ultra-capacitor is represented by internal resistances (R_s and R_p) and capacitance (C_{uc}). It functions as a secondary energy storage device that is capable of delivering or absorbing high power during transient conditions. The ultra-capacitor and the converter are connected by an inductor (L_2), which facilitates controlled energy transfer and smooths current. The bidirectional power conversion path between the UC and the DC bus is

formed by a diode, two primary switching devices (Q2 and Q3), and the circuit. The inductor and switching devices transfer the stored energy in the ultra-capacitor to the DC bus during boost mode (discharging of UC), thereby increasing the DC bus voltage to supply the load. The ultra-capacitor is able to store excess energy by permitting energy to flow from the DC bus back to it in buck mode (charging of UC). The voltage and current flow in both directions are regulated by the toggling operation.

In order to mitigate ripple and preserve a consistent DC voltage, a DC bus capacitor (C_{bus}) is connected across the load. The DC bus supplies the capacity, guaranteeing uninterrupted power delivery. In general, this topology is well-suited for applications such as regenerative braking systems, hybrid energy storage systems, and electric vehicles, as it facilitates efficient bidirectional energy flow, rapid transient response, and enhanced system stability.

The design of non-isolated bidirectional DC-DC converters has been the subject of numerous studies in the literature. For example, [3] emphasizes the performance parameters of buck-boost, single-ended primary inductor, Cuk, z-source, zeta, and hybrid DC-DC converters, which are all examples of current and future trends in non-isolated converters. The design and control of a multiphase gap bidirectional DC-DC converter were conducted in [4]. A bidirectional DC-DC converter (BDC) is suggested for the EV application in [5]. An investigation is conducted in [6] into a hybrid modular DC-DC converter that is bidirectional, non-isolated, and designed for high voltage (HV) applications. A bidirectional DC-DC converter with dual input terminals for Hybrid Energy Storage Systems (HESS) is the subject of an additional study [7]. The research [8] concentrates on the modified structure of power electronic interfaces that are capable of being utilised in electric vehicle (EV) applications. These interfaces feature four non-isolated ports, including two input and two output ports. A comprehensive review of non-isolated bidirectional DC-DC converter topologies is provided in another study [9]. In [10], a bidirectional DC-DC converter that is simplified, non-isolated, and based on logic control circuits is proposed for both battery and super capacitor topologies. An additional investigation suggests that an enhanced non-isolated single inductor multiple input buck DC-DC converter with a reduced component count exists [11]. A new bidirectional multi-port DC-DC converter is introduced in [12] and is recommended for EV applications. This converter can be operated in both step-up and step-down modes. An advanced controller for multi-input bidirectional DC-DC power converters designed for hybrid energy storage systems (HESS) is introduced in an additional study [13]. A novel non-isolated bidirectional DC-DC converter with zero voltage switching (ZVS) capability and free fluctuation input current is proposed in [14].

A novel integrated cascade bidirectional DC-DC converter is introduced in another paper to enhance a central charge balancing system [15]. The performance analysis and comparison of two varieties of bidirectional DC-DC converters, a step-down-booster capacitor in the middle and a step-down-step-up inductor in the middle, for use in EVs are presented in [16]. Another study examined a potential EV configuration that utilised a bidirectional DC-DC converter to facilitate reliable and rapid energy transfer, utilizing supercapacitors and batteries [17].

A novel topology for high-stage multiport DC-DC converters is introduced in [18].

A power electronic device known as a bidirectional DC-DC converter is highly suitable for vehicle applications that require the supply and recovery of energy. This is due to the fact that it enables power to travel in both directions. It is primarily employed in electric vehicles to facilitate the efficient transmission of energy during both regenerative braking and driving conditions by interfacing the battery, supercapacitor, and DC bus.

During normal driving or acceleration, the converter operates in boost mode, transferring energy from the battery (low voltage side) to the DC bus (high voltage side) to power the motor. In contrast, it operates in buck mode during regenerative braking, which enables the conversion and storage of energy from the motor back into the battery. This bidirectional capability enhances the overall efficacy of energy and prolongs the lifespan of batteries. EDVs (Electric Drive Vehicles) employ the fundamental concept of vehicle-to-grid power to supply electric power to the grid while the vehicle is stopped. The EDV may be a plug-in hybrid vehicle, a fuel cell vehicle, or a battery-electric vehicle. Plug-in hybrid EDVs are capable of operating in either mode. Regardless of whether they are powered by batteries, fuel cells, or petrol hybrids, EDVs contain the stored energy in the battery and power converters that are capable of generating a 50 Hz AC voltage that supplies electricity to our residences and offices. V2G (Vehicle to Grid) is the term used to describe the process of establishing connections to facilitate the transmission of electricity from vehicles to power lines. When connections are implemented to recharge the battery of EDVs from power lines, the term "G2V" (Grid to Vehicle) is used.

Traditional vehicles are being replaced by plug-in hybrid electric vehicles (PHEVs). The concept of a smart grid is visualized through the transmission of energy from the grid to the vehicle and from the vehicle to the grid. One can generate revenue by transferring energy from a plug-in hybrid electric vehicle (PHEV) to the grid during peak hours and reclaiming it from the grid during lean hours. This is due to the fact that the cost of energy is significantly higher during peak hours than during lean hours. The battery of an electric vehicle contains a significant quantity of energy. One typical EDV has the capacity to produce over 10 kW, which is equivalent to the average drawn power of ten households. The precise timing of grid power production to align with driving requirements and satisfy the time-critical power "dispatch" of the electric distribution system is the critical factor in achieving economic value from V2G. Grid electricity is employed by plug-in hybrid electric vehicles (PHEVs) to replace the consumption of transportation fuel. The battery is a critical component of the efficacy of plug-in hybrid electric vehicles (PHEVs). It is imperative to ensure that the battery is charged and discharged efficiently in order to preserve its reliability, safety, and longevity. The system is capable of charging batteries at a rate of up to 10A. It is also capable of supplying energy to the 230V, 50 Hz single-phase power at a rate of 10A. A single-phase bidirectional AC-DC converter and a DC-DC converter comprise the system. The purpose of a single-phase bidirectional AC-DC converter is to convert AC voltage to DC voltage. In buck mode, the buck-boost DC-DC converter is employed to charge the battery, while in boost mode; it is

employed to discharge the battery. This system's feasibility is illustrated by the battery's charging and discharging cycles [20-21].

II RELATED WORK

Table 1 Literature Review Table: Bidirectional DC-DC Converter & EV Charging Systems

| S. No. | Author & Year | Objective | Methodology / Technique | Key Findings | Limitations / Research Gap |
|---------------|---------------------------------|---|--|---|---|
| 22 | M. P. Mohandass et al. (2025) | To develop an efficient EV fast charging system using Vienna rectifier topology | Hybrid EJS-RDF (Enhanced Jellyfish Search + Random Decision Forest), AC-DC Vienna Rectifier with buck/boost converters | Achieved low THD (3.50% G2V, 3.80% V2G), improved power factor, optimized duty cycle, enhanced efficiency | Complexity of hybrid algorithm; requires high computational resources |
| 23 | R. Islam et al. (2023) | To review power converter technologies for EV applications | Comparative analysis of AC-DC, DC-DC, and DC-AC converters; study of control methods and materials (GaN, etc.) | Identified Vienna rectifier as best AC-DC converter; highlighted interleaved DC-DC boost converter and multilevel inverter benefits | Lacks experimental validation; mostly theoretical review |
| 24 | S. K. Paramasivam et al. (2025) | To improve power quality in fast EV charging stations | T-Type Vienna Rectifier (3P3L4W) with IIPQ control and fuzzy logic | Achieved low THD (~2.5%), improved dynamic response, reduced switching losses, enhanced stability | Hardware complexity and cost; limited scalability discussion |
| 25 | S. B. Kumbhar et al. (2024) | To analyze optimization techniques for controller | Review of PID, MPC, SMC, fuzzy logic with optimization | Optimization improves stability, robustness, and | No specific implementation or case study validation |

| | | | | | |
|----|--------------------------|---|--|--|---|
| | | performance in EV systems | algorithms (PSO, GA, Lyapunov) | control accuracy in nonlinear systems | |
| 26 | M. M. Rana et al. (2024) | To review EV charging technologies and their impact on the power grid | Comparative study of charging methods (slow/fast, wireless), converter types, and grid interaction | Identified challenges like cost, grid stability, THD, and efficiency; highlighted smart grid integration | Needs practical models for real-time implementation |

III PROPOSED SYSTEM IMPLEMENTATION

The basic concept of vehicle-to-grid power is used in EDVs (Electric Drive Vehicles) to provide electric power to the grid while the vehicle is parked. The EDV can be a battery–electric vehicle, fuel cell vehicle, or a plug-in hybrid vehicle. Plug-in hybrid EDVs can function in either mode of operation. EDVs, whether powered by batteries, fuel cells, or gasoline hybrids, have within them the stored energy in the battery and power converters capable of producing a 50 Hz AC voltage that powers our homes and offices. When connections are added to allow this electricity to flow from cars to power lines, one calls it V2G (Vehicle to Grid). When connections are added to charge the battery of EDVs from power lines, then it is termed as G2V (Grid to Vehicle). PHEVs (Plug-in Hybrid Electric Vehicles) are emerging as replacement for traditional vehicles. With the energy transfer from the grid to vehicle and vehicle to grid, the concept of smart grid is visualized. One can transfer energy from PHEV to grid when it is parked in peak hours and can take energy back from the grid in lean hours, thereby can earn some revenue as the cost of energy is much more in peak hours than in lean hours. An electric vehicle pack has a substantial amount of energy stored in its battery. One typical EDV can output over 10 kW, the average drawn power of 10 houses.

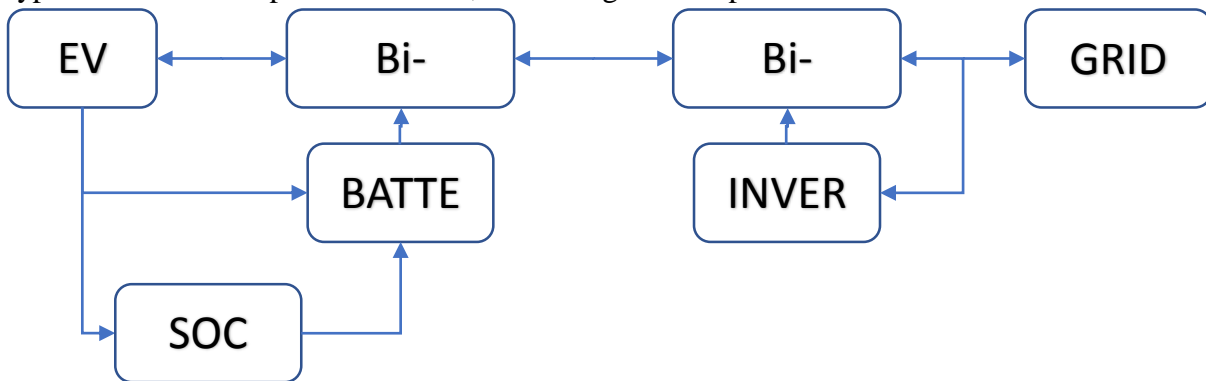


Fig.2 Proposed Block Diagram

The key to realizing economic value from V2G is precise timing of its grid power production to fit within driving requirements while meeting the time-critical power “dispatch” of the

electric distribution system. PHEVs use grid electricity to displace transportation fuel consumption. The battery plays an important role in the performance of PHEVs. Efficient charging and discharging of the battery are essential to maintain good battery life, safety, and reliability. In this paper, a configuration with the bidirectional power converters is derived for the bidirectional power management of a PHEV battery. The system can charge battery up to 10A current. It can also deliver energy back to the 230V, 50 Hz single-phase power at 10A rate. The system is composed of two parts: a single-phase bidirectional AC-DC converter and a DC-DC converter. Single-phase bidirectional AC-DC converter is to convert AC to DC voltage. The buck-boost DC-DC converter is used in buck mode for charging and a boost mode when discharging the battery. The charging and discharging of the battery demonstrate the feasibility of the system.

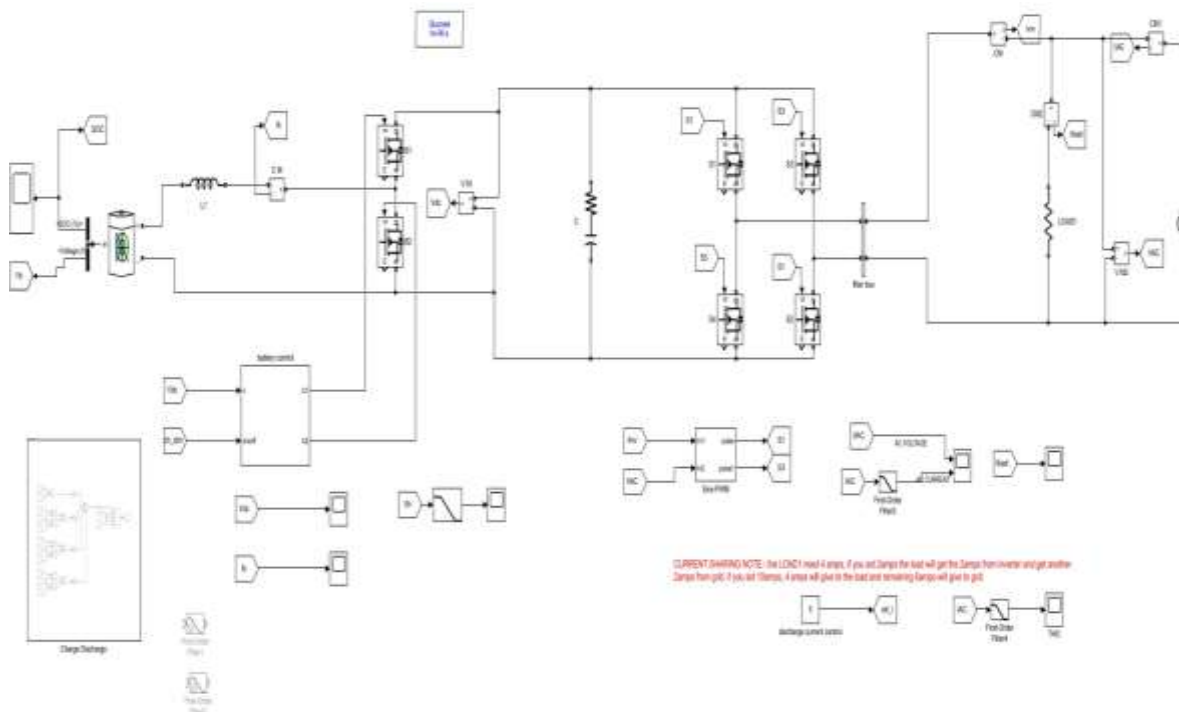


Fig.3 Proposed Simulink Model

figure 3 represents a battery-based power electronic conversion system modeled in MATLAB/Simulink, where DC power from a battery is converted into a controlled AC output for supplying a load. Initially, the battery acts as the primary DC source, and its performance is monitored through parameters like state of charge and current measurement. The DC power then passes through an inductor, which helps in smoothing current fluctuations, and enters a DC-DC converter stage consisting of controlled switching devices such as IGBTs or MOSFETs. This stage regulates the voltage level and manages the charging and discharging behavior of the battery. The output of this converter is fed into a DC link capacitor, which stabilizes the DC voltage and reduces ripples, ensuring a steady supply for the next stage. Following this, the stabilized DC is converted into AC using an H-bridge inverter composed of four switches (S1-S4), which are controlled by a sine pulse width modulation (PWM) technique to generate a sinusoidal waveform. The inverter output is then passed through an LC

filter to eliminate harmonics and produce a smooth AC signal suitable for the load. Measurement blocks are incorporated to monitor AC voltage and current, often processed through filters for accurate analysis. The system also includes a control unit that continuously adjusts switching signals based on feedback to maintain stable operation under varying load conditions. Additionally, the diagram highlights a current-sharing mechanism, where both the battery and inverter cooperate to meet load demands, enhancing system efficiency and preventing overload. Overall, the system functions as an efficient DC–AC power conversion unit commonly used in applications such as UPS systems, renewable energy systems, and microgrids. Implements a generic battery model for most popular battery types. Temperature and aging (due to cycling) effects can be specified for Lithium-Ion battery type.

Table 2 Battery Parameters

| Variable | Parameters Value |
|-------------------------------------|------------------|
| Nominal voltage (V) | 150 |
| Rated capacity (Ah) | 15 |
| Initial state-of-charge (%) | 40 |
| Battery response time (s) | 30 |
| Maximum capacity (Ah) | 15 |
| Cut-off Voltage (V) | 112.5 |
| Fully charged voltage (V) | 174.5981 |
| Nominal discharge current (A) | 6.5217 |
| Internal resistance (Ohms) | 0.1 |
| Capacity (Ah) at nominal voltage | 12.56 |
| Discharge current [i1, i2, i3,] (A) | [6.5 13 32.5] |

MOSFET and internal diode in parallel with a series RC snubber circuit. When a gate signal is applied the MOSFET conducts and acts as a resistance (R_{on}) in both directions. If the gate signal falls to zero when current is negative, current is transferred to the antiparallel diode.

Table 3 MOSFET Parameters

| Variable | Parameters Value |
|---|------------------|
| FET resistance R_{on} (Ohms) : | 0.1 |
| Internal diode resistance R_d (Ohms) : | 0.01 |
| Snubber resistance R_s (Ohms) : | 1e5 |

PID -This block implements continuous- and discrete-time PID control algorithms with setpoint weighting and includes advanced features such as anti-windup, external reset, and signal tracking. You can tune the PID gains automatically using the 'Tune...' button (requires Simulink Control Design)

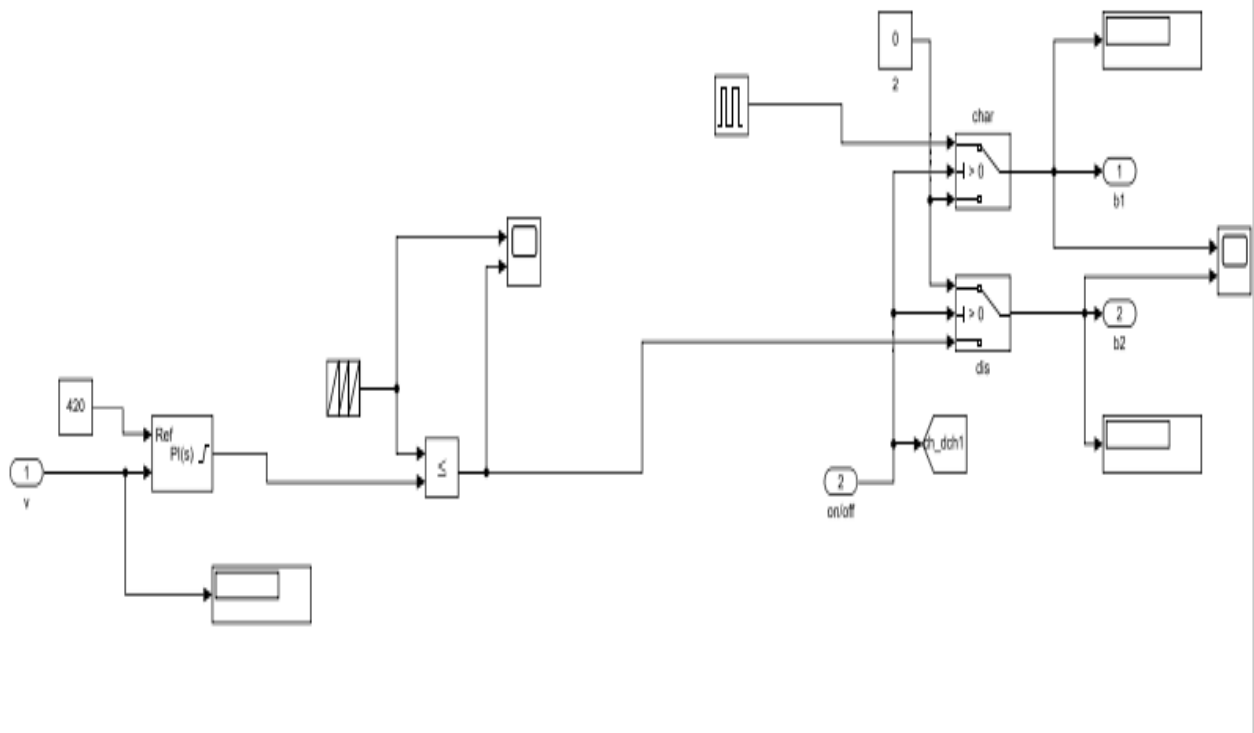


Fig. 4 PID Control Block

The figure 4 represents a control system model implemented in MATLAB/Simulink for regulating voltage using a closed-loop feedback mechanism. The system takes an input voltage and compares it with a reference value (set at 420 V), and the error signal is processed through a PI (Proportional–Integral) controller to generate a control signal. This signal is then compared with a high-frequency carrier waveform to produce switching pulses using a PWM (Pulse Width Modulation) technique. The generated pulses are further processed through logical and switching blocks to control the operation of power electronic switches. The model includes enable/disable (on/off) control logic and signal routing blocks that determine the activation of different switches (b1 and b2), ensuring proper system operation. Display and scope blocks are used for monitoring system outputs.

Control of Single-Phase

Bidirectional AC-DC Converter In the control of single-phase bidirectional AC-DC converter, a unipolar switching scheme is used, in which the triangular carrier waveform is compared with two reference signals which are positive and negative signals. The output voltage varies between 0 and Vdc, or between 0 and –Vdc.

- The PID voltage controller closely tracks the reference voltage (Vref) and gives a control signal (Ip) to minimize the voltage error Ve (k) which is calculated from the reference voltage Vref (k) and a sensed voltage Vdc(k) at kth instant of time as,
- $V_e(k) = V_{ref}(k) - V_{dc}(k)$
- The output of the controller $I_p(k)$ at kth instant is given as,
- $I_p * (k) = I_p * (k-1) + K_{pv} \{ V_e(k) - V_e(k-1) \} + K_{iv} V_e(k)$ (10)
- where K_{pv} and K_{iv} are the proportional and integral gains of the voltage controller.

- The PI current controller closely tracks the reference current $I_p^*(k)$ and gives a control signal V_{cs} to minimize the current error $I_e(k)$ which is calculated from the reference current $I_p^*(k)$ and a sensed current $I_p(k)$ at k th instant of time as, $I_e(k) = I_p^*(k) - I_p(k)$ (11)
- This current error is amplified using the proportional controller by gain “K,” and which is given as, $V_{cs} = kI_e(k)$ (12)
- This amplified signal is compared with fixed-frequency (10 kHz) triangular carrier wave in unipolar PWM switching signals for the IGBTs of single-phase bidirectional AC-DC converter [7].

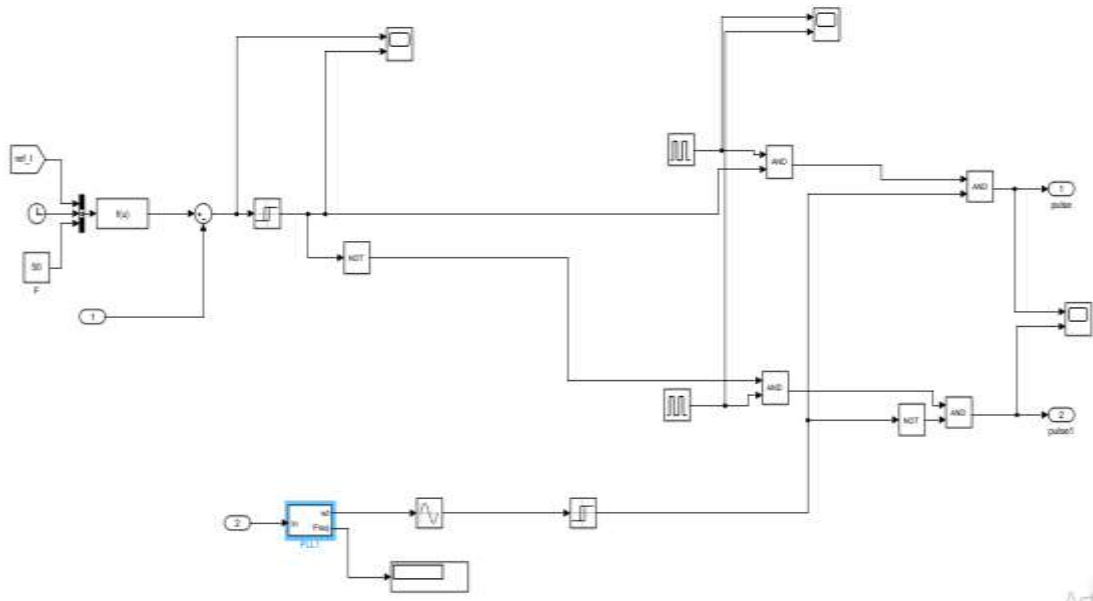


Fig.5 PWM modulator

PWM modulator -The performance of the converter depends on both the modulation strategy and the switching pattern arrangement. In this paper, reducing the switching power losses and output current ripple are the main consideration when arranging the switching pattern. Therefore, a symmetrical switching pattern is usually applied [20]. Both the front-end switching pattern and the rear-end switching pattern need to be arranged. In addition, coordination control between the front-end switching pattern and the rear-end switching pattern is required., the in-phase carrier PWM modulator is adapted under the charging operation, and the interleaved carrier PWM modulator is adapted under the discharging operation. which illustrates the specific operation of each switch in each switching period. show the changes of the voltage across inductor L and the dc current i_{dc} . Here the voltage drops across the IGBTs and the diodes are neglected. From Fig.5.4 the switching patterns are bilaterally symmetrical, and twice commutations occur in each switching period

PLL

This Phase Locked Loop (PLL) system can be used to synchronize on a variable frequency sinusoidal signal. When the Automatic Gain Control is enabled, the input (phase error) of the PLL regulator is scaled according to the input signal magnitude.

For optimal performance, set regulator gains [Kp Ki Kd] = [180 3200 1] and check the Enable Automatic Gain Control parameter.

- Input: Normalized input signal (pu)
- Output 1: Measured frequency (Hz) = w/(2pi)
- Output 2: Ramp w.t varying between 0 and 2*pi, synchronized on the zero-crossing (rising) of the fundamental of input signal

SOC

SOC control circuit limits the rate at which electric current is added to or drawn from electric batteries to protect against electrical overload, overcharging, and may protect against overvoltage. This prevents conditions that reduce battery performance or lifespan and may pose a safety risk. It may also prevent completely draining ("deep discharging") a battery, or perform controlled discharges, depending on the battery technology, to protect battery life. The terms "charge controller" or "charge regulator" may refer to either a stand-alone device, or to control circuitry integrated within a battery pack, battery-powered device, or battery charge. The SoC is a relative quantity that describes the ratio of the remaining capacity to the present maximum available capacity of a battery, and it is given by

$$SoC_t = SoC_0 - \int_0^t \eta_i I_{L,t} dt / C_a \quad \text{Eq.1}$$

where SoC_t is the present SoC, SoC₀ is the SoC initial value, I_{L,t} is the instantaneous load current (assumed positive for discharge, negative for charge), η_i is the Coulomb efficiency, which is the function of the current and the temperature; and C_a is the present maximum available capacity, which may be different from the rated capacity for the age effect.

$$SoC_k = SoC_{k-1} - \eta_i I_{L,k} \Delta_t / C_a \quad \text{Eq.2}$$

Where Δ_t is the sampling period (in hours). Eq. (5.2) provides a basis to calculate the SoC with SoC_{k-1} and current I_{L,k} at the kth sample time in a state equation format. The battery model will then be differentiated by the additional components in the state vector and the functional form of f(x, u) and g(x, u).

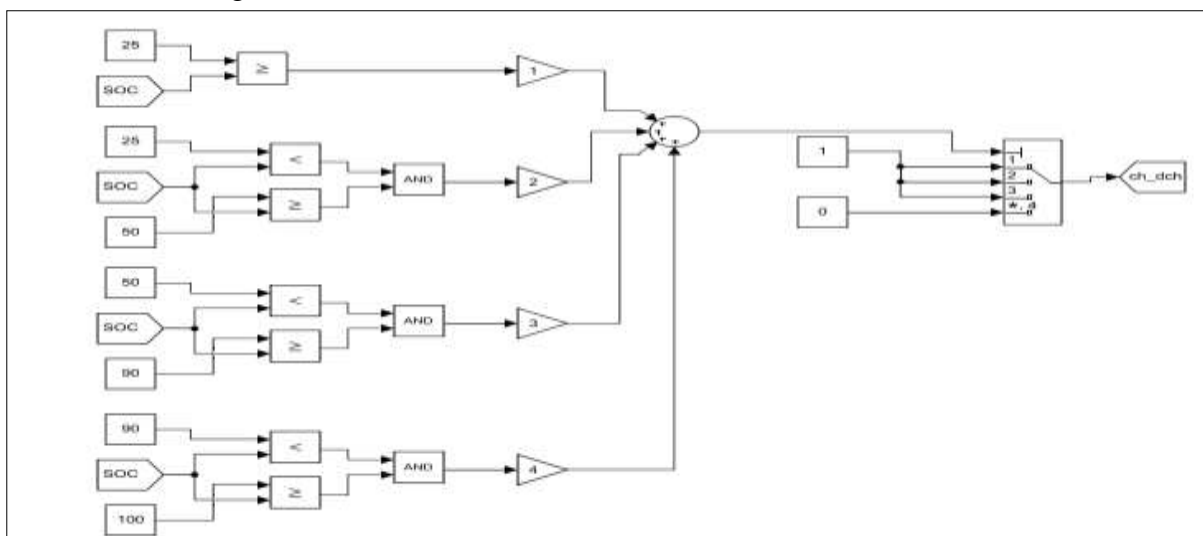


Fig.6 SOC control circuit

IV SIMULATION RESULTS

To validate the proposed topology and method, simulations based on the Matlab/Simulink environment are implemented in this section. The models of the semiconductor devices and battery are from the SimPowerSystems/Power Electronics library. A schematic diagram of the single-phase current source bidirectional converter in the simulation is shown in Fig.1. The loads are 15Ah capacity lead-acid battery with nominal voltage of 150V.

Different soc charging condition performed in the simulation

- If soc less than 25, it will charge
- If soc between 25 to 50, it will charge
- If soc between 50 to 90, it will charge
- If soc between 90to 100, it will discharge

Table 4 SOC Charging condition

| NO.1 | SOC | Status | Action |
|------|------------------|------------------|---|
| 1 | Less than 25% | charge | Disconnected from load only charging of battery |
| 2 | 25 % < SOC < 50% | charge | V2G avoided charging done |
| 3 | 50% < SOC < 50% | charge | Vehicle to grid perform ,charging |
| 4 | SOC = 100% | discharge | Grid perform ,no charging |

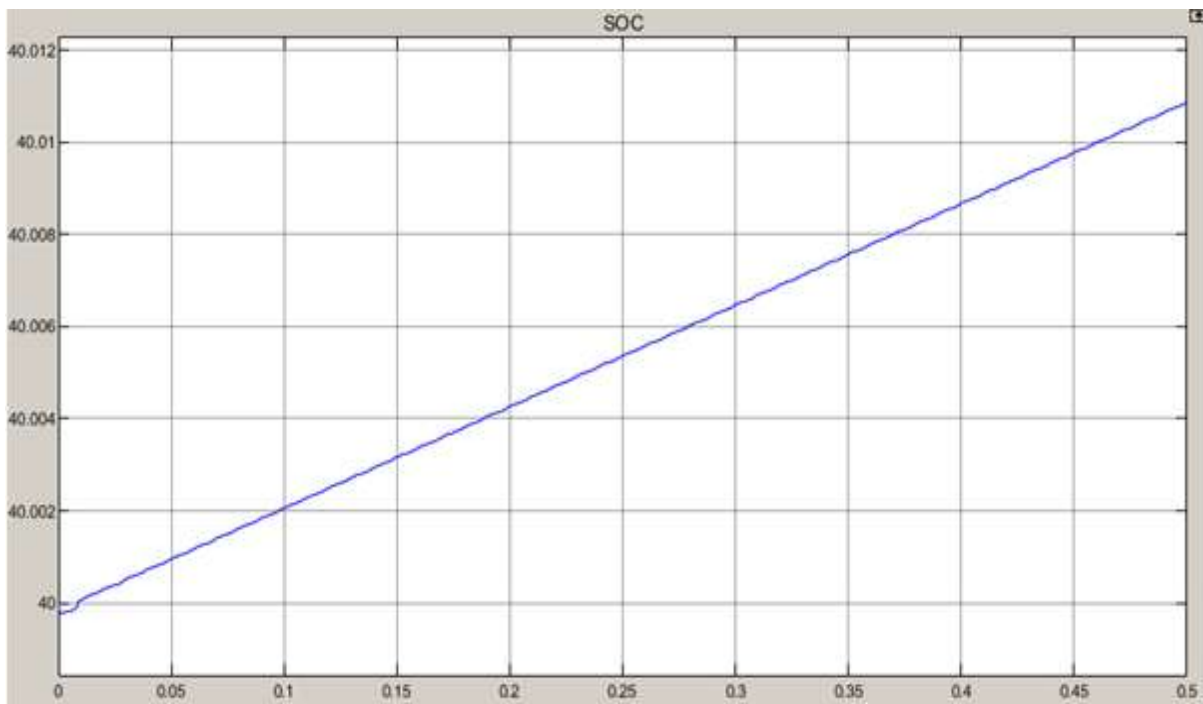


Fig.7 SOC charging at 40%

In the simulation 4 SOC condition check to check the SOC of the battery in the first case If soc between 0 to 25%, it will charge showing in fig 7



Fig.8 SOC charging at 50%

In the third case If soc between 50% to 90%, it will charge showing in fig.8

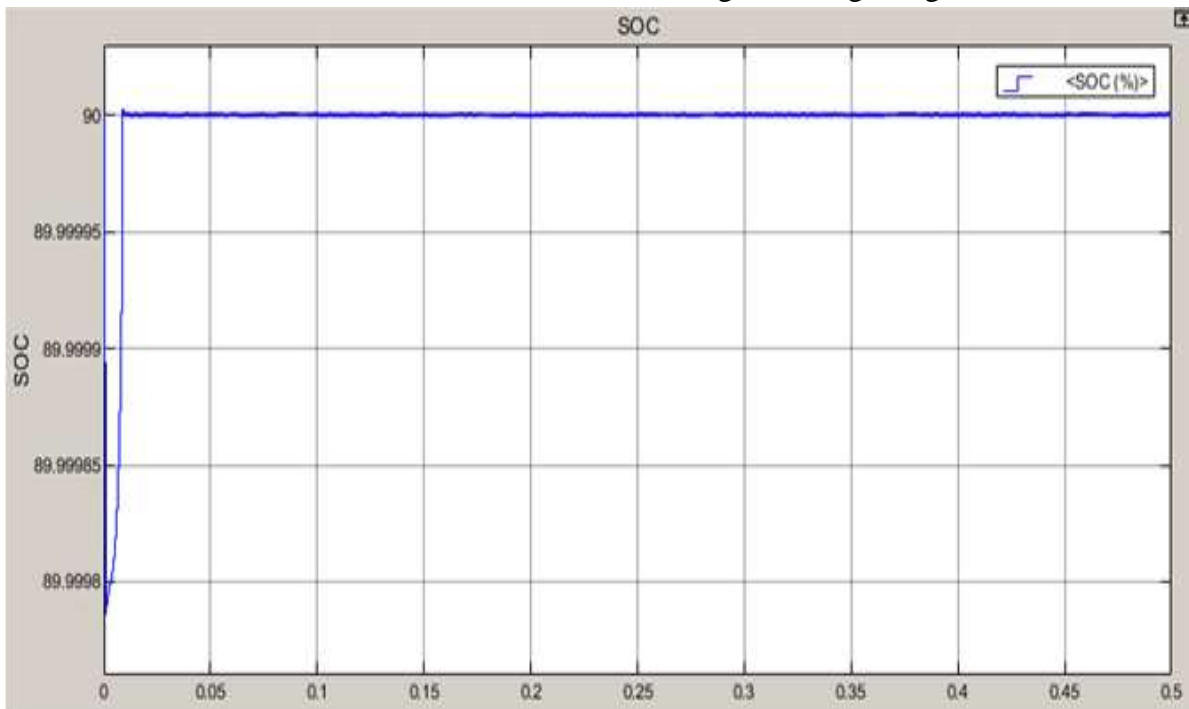


Fig.9 SOC charging at 90%

In the third case If soc between 50% to 90%, it will charge showing in fig. 9

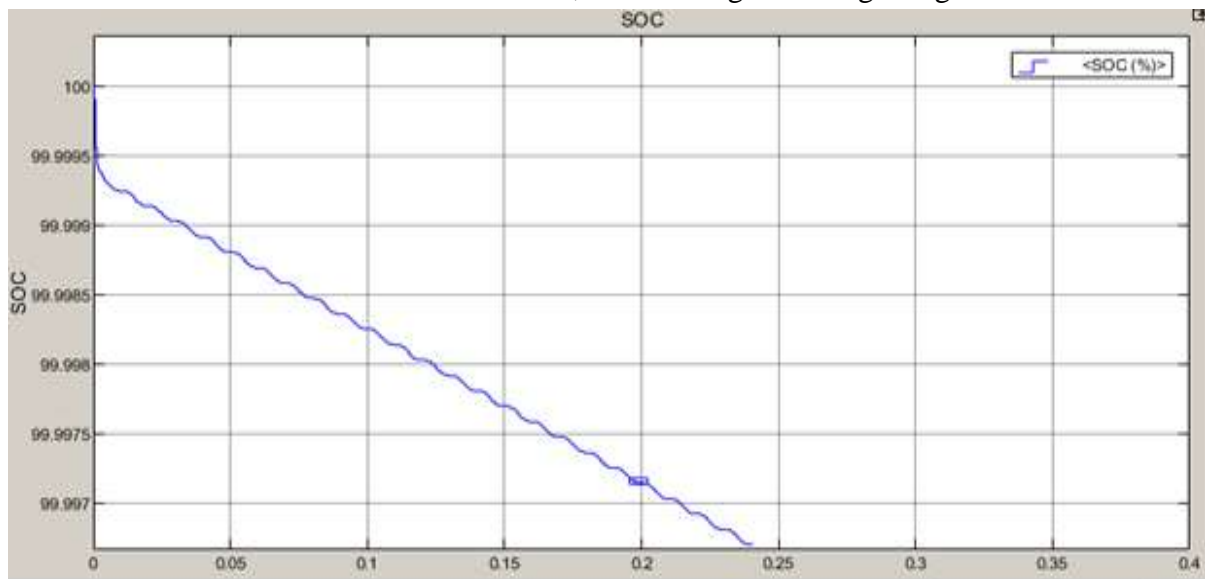


Fig.10 SOC discharging at 100%

In fourth case If soc between 90 to 100, it will discharge showing in fig. 10

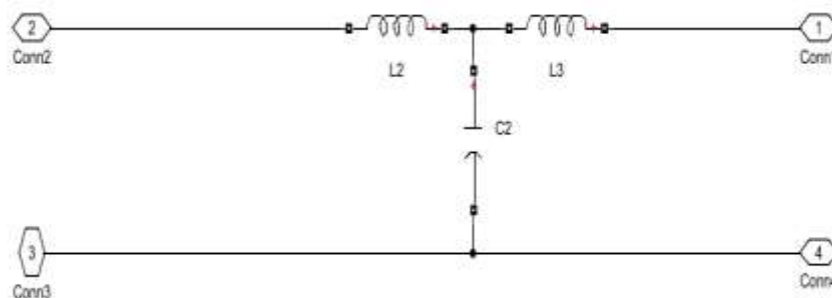


Fig.11 Filter Block

Implement a first-order filter.

- Filter type = Lowpass -> $H(s) = 1/(1+T.s)$
- Filter type = Highpass -> $H(s) = T.s/(1+T.s)$

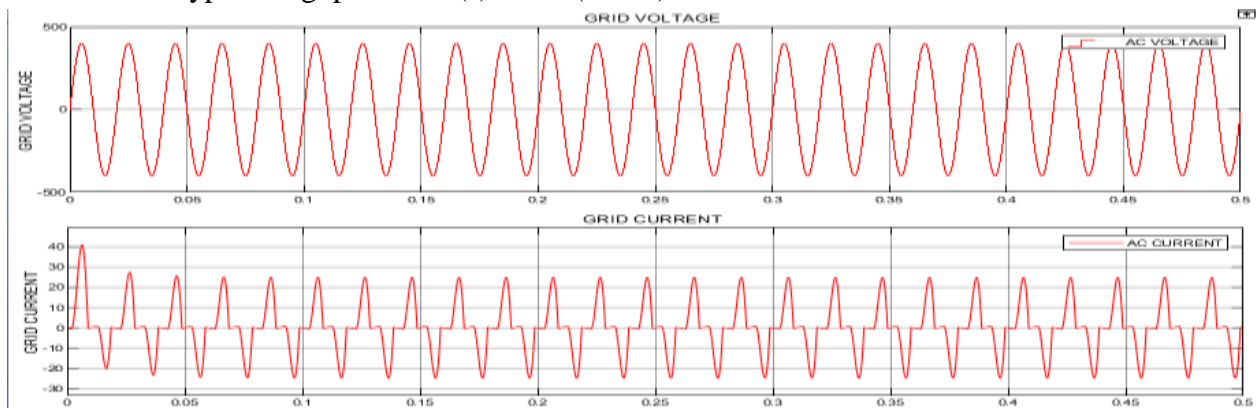


Fig.12 Grid current and voltage

The grid voltage waveform exhibits a pure sinusoidal pattern, indicating a stable and well-regulated AC supply. The amplitude remains nearly constant throughout the time period, showing that there are no significant disturbances, fluctuations, or distortions in the voltage. This reflects proper synchronization of the inverter with the grid and ensures high power quality.

The grid current waveform shows a pulsating and slightly distorted pattern compared to the voltage waveform. This indicates the presence of switching effects due to power electronic devices such as inverters. Although the current follows the general sinusoidal trend, the spikes and ripples suggest harmonic components in the system. These distortions can be reduced using appropriate filtering techniques.

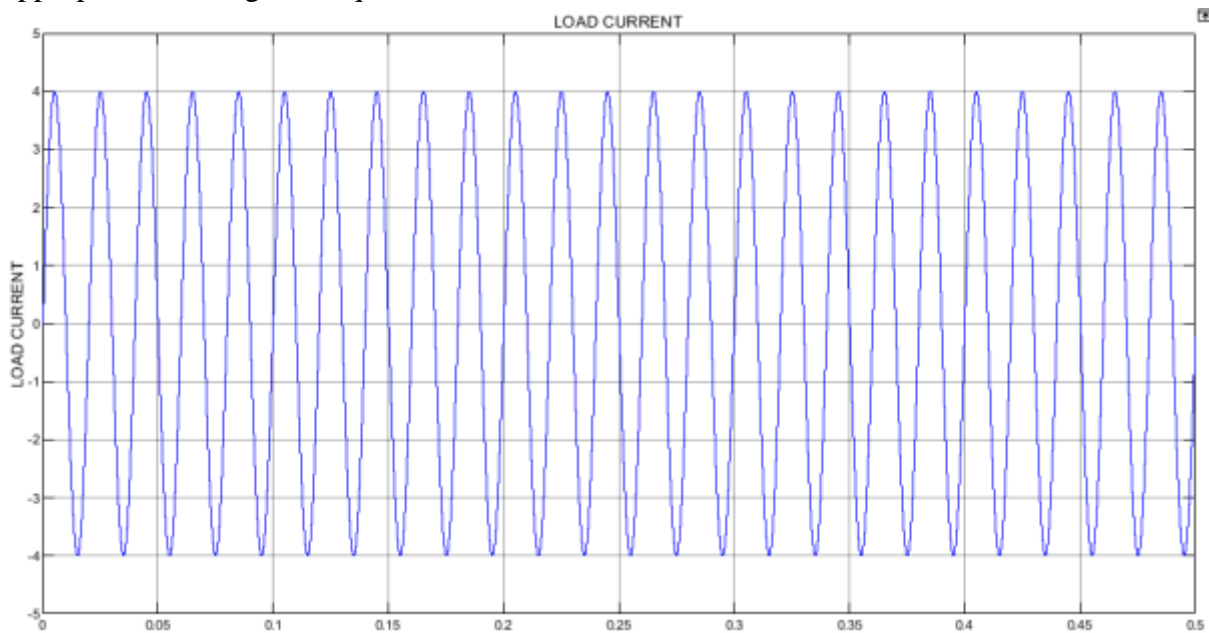


Fig.13load current

The load current waveform shows a nearly sinusoidal pattern with consistent amplitude over time. The waveform is smooth and periodic, indicating that the load is receiving a stable AC current. Minor ripples may be present due to switching operations, but overall the current quality is good, reflecting effective filtering and proper inverter operation.

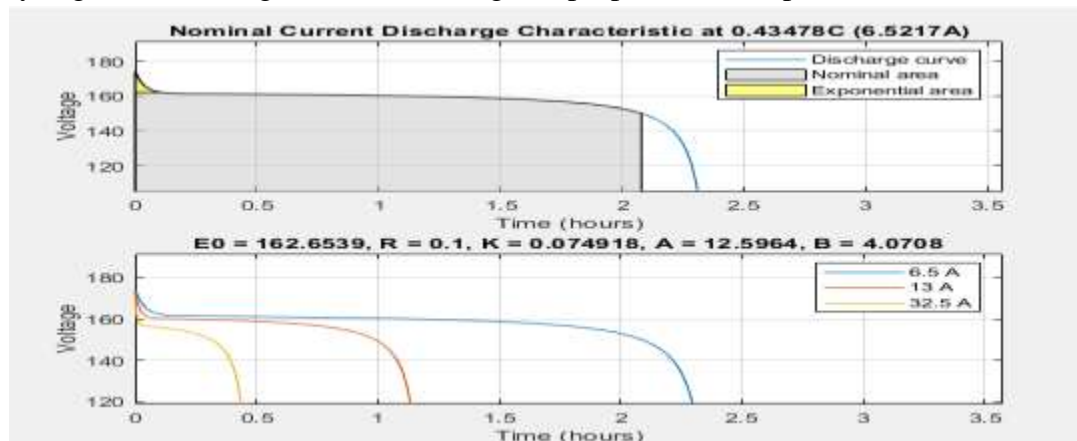


Fig.14 battery discharging characteristics

This figure illustrates the discharge behavior of the battery under different current levels. The voltage gradually decreases over time as the battery discharges. Higher discharge currents result in a faster drop in voltage and reduced discharge duration, while lower currents maintain the voltage for a longer period. This demonstrates the dependency of battery performance on load conditions.

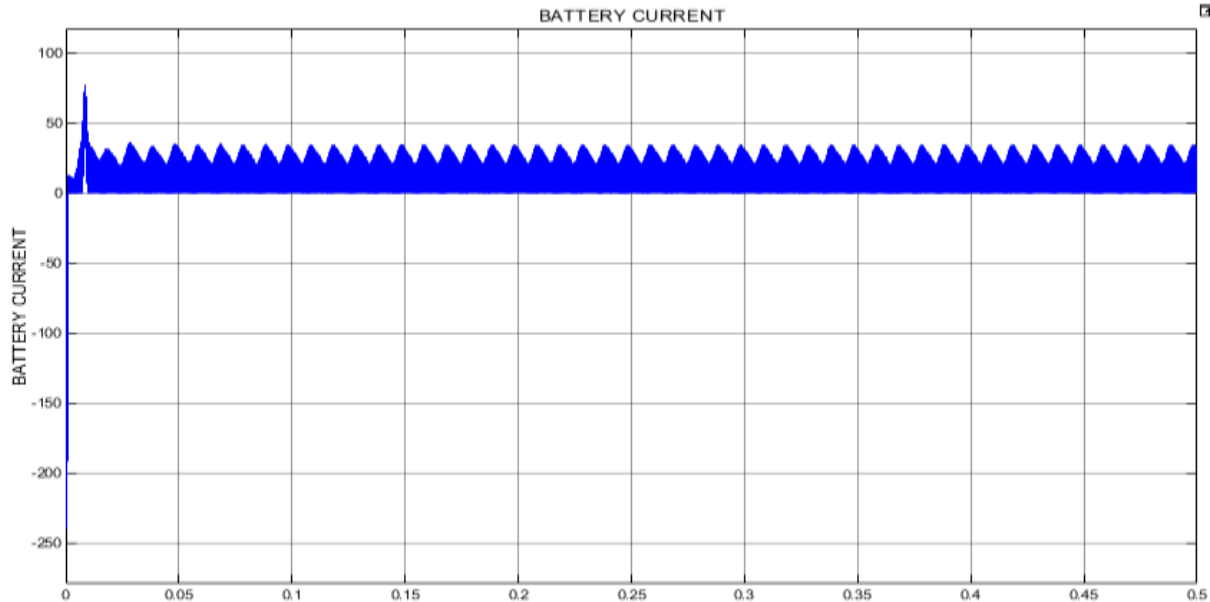


Fig.15 battery voltage

The battery current waveform shows a controlled and continuous current profile with small oscillations. The fluctuations are due to switching actions of the converter, but the overall current remains stable. This indicates proper current regulation and efficient energy transfer between the battery and the system.

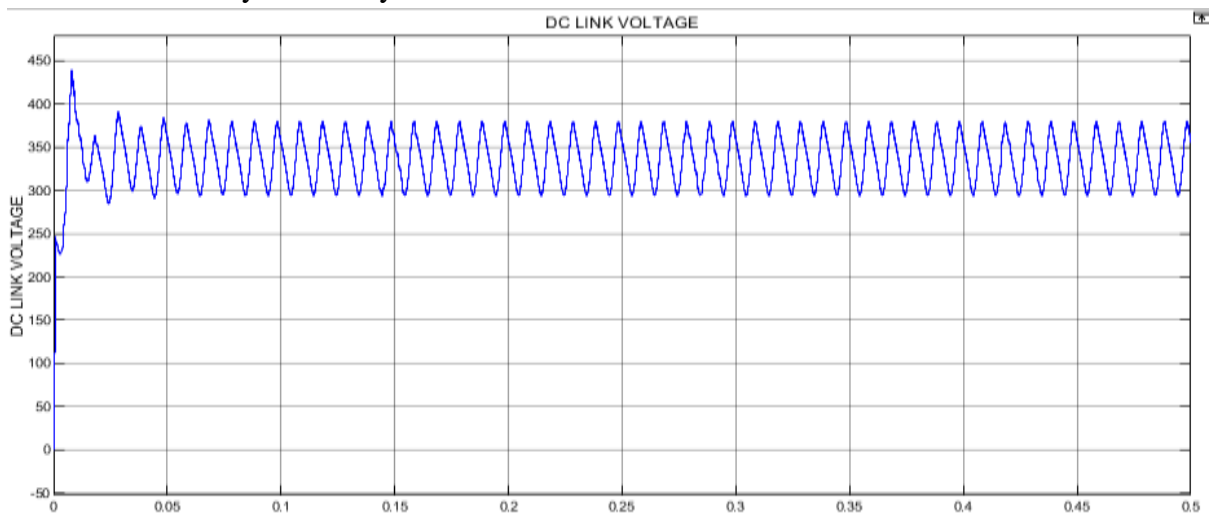


Fig.16 DC link voltage

The DC link voltage waveform shows a relatively constant voltage level with small ripples. The ripples are caused by switching in the power electronic devices, but they are well within acceptable limits. This confirms that the DC link capacitor is effectively maintaining voltage stability and ensuring smooth power flow to the inverter.

Table 5 Performance Analysis Table

| Parameter | Observed Value (Approx.) | Waveform Nature | Performance Interpretation |
|----------------------|--------------------------|----------------------|---|
| SOC (40%) | 40% → 40.12% | Linear Increasing | Stable and efficient charging at low SOC |
| SOC (50%) | 50% → 50.03% | Gradual Increasing | Moderate charging with controlled rate |
| SOC (90%) | 90% (constant) | Saturation | Charging slows to prevent overcharging |
| SOC (100%) Discharge | 100% → 99.97% | Gradual Decreasing | Smooth and controlled discharging |
| Grid Voltage | ±400–450 V | Pure Sinusoidal | High power quality, stable grid synchronization |
| Grid Current | ±20–40 A | Pulsating/Distorted | Switching harmonics present |
| Load Current | ±4 A | Near Sinusoidal | Good filtering and stable load supply |
| Battery Current | 0–30 A | Slight Ripple | Controlled charging/discharging |
| DC Link Voltage | 300–350 V | Constant with Ripple | Stable DC bus, effective capacitor filtering |
| Battery Voltage | 150–160 V | Slowly Decreasing | Normal discharge characteristics |

Table 5 present a MATLAB/Simulink simulation results are used to evaluate the proposed bidirectional DC–DC converter system in Table 2. The table lists electrical parameters, their observed values, waveform features, and performance interpretations. At lower levels (40% and 50%), the battery charges steadily and efficiently, as shown by the linear and gradual increase in SOC. Saturation slows charging to prevent overcharging and improve battery safety as SOC exceeds 90%. Discharging at 100% SOC shows a progressive decline, showing stable energy delivery. The grid voltage waveform is sinusoidal within ±400–450 V, indicating high power quality and grid synchronisation. However, switching harmonics from power electronic equipment cause the grid current to pulse and distort, highlighting the necessity for better filtering in actual systems. The load current is virtually sinusoidal, with a steady amplitude of ±4 A, indicating that the inverter and output filter successfully reduce harmonics and ensure reliable supply. The battery current fluctuates between 0–30 A with small ripples, indicating controlled charging and discharging with acceptable switching effects. The DC link capacitor keeps the DC link voltage steady between 300–350 V with minor ripples, ensuring smooth power transfer. Last, during discharge, the battery voltage gradually decreases between 150–160 V, which is normal under load.

V CONCLUSION

The proposed converter has delivered the AC current to/and from the grid at unity power factor and at very low current harmonics which ultimately prolongs the life of the converter and the

battery and minimizes the possibility of distorting the grid voltage. It also enables V2G interactions which could be utilized to improve the efficiency of the grid. The proposed converter has delivered the AC current to/and from the grid at unity power factor and at very low current harmonics which ultimately prolongs the life of the converter and the battery and minimizes the possibility of distorting the grid voltage. The simulation results confirm that the system maintains a stable DC link voltage and delivers high-quality AC output to the load. The SOC analysis shows that the battery charges efficiently at lower levels and adopts a controlled charging mechanism near full capacity, preventing overcharging. During discharging, the battery provides a smooth and continuous power supply to the load. The grid voltage waveform remains purely sinusoidal, ensuring good power quality and synchronization, while the grid current exhibits minor harmonic distortions due to switching operations. The load current remains stable and nearly sinusoidal, indicating effective filtering and proper inverter performance.

VI REFERENCES

1. F. Üstünsoy and H. H. Sayan, "Real-time realization of network integration of electric vehicles with a unique balancing strategy," *Electrical Engineering*, vol. 103, pp. 2647–2660, 2021.
2. S. Yildiz and H. H. Sayan, "LCL Filter Design and Simulation for Vehicle-To-Grid (V2G) Applications," in *Proc. IMSS 2023*, 2024.
3. F. Mumtaz, N. Z. Yahaya, S. T. Meraj, B. Singh, R. Kannan, and O. Ibrahim, "Review on non-isolated DC-DC converters and their control techniques for renewable energy applications," *Ain Shams Engineering Journal*, vol. 12, no. 4, pp. 3747–3763, 2021.
4. A. Sahbani, K. Cherif, and K. B. Saad, "Multiphase Interleaved Bidirectional DC-DC Converter for Electric Vehicles and Smart Grid Applications," *International Journal of Smart Grid*, vol. 4, no. 2, pp. 80–87, 2020.
5. R. Rezaei, M. Nilian, M. Safayatullah, S. Ghosh, and I. Batarseh, "A Bidirectional DC-DC Converter with High Conversion Ratios for Electrical Vehicle Application," in *IECON 2021 – 47th Annual Conf. IEEE Industrial Electronics Society*, pp. 1–6, 2021.
6. [6] A. Elserougi, I. Abdelsalam, A. Massoud, and S. Ahmed, "A bidirectional non-isolated hybrid modular DC–DC converter with zero-voltage switching," *Electric Power Systems Research*, vol. 167, pp. 277–289, 2019.
7. [7] F. D. Hernandez, R. Samanbakhsh, P. Mohammadi, and F. M. Ibanez, "A dual-input high-gain bidirectional DC/DC converter for hybrid energy storage systems in DC grid applications," *IEEE Access*, vol. 9, pp. 164006–164016, 2021.
8. K. Suresh et al., "A multifunctional non-isolated dual input–dual output converter for electric vehicle applications," *IEEE Access*, vol. 9, pp. 64445–64460, 2021.
9. N. A. Al-Obaidi, R. A. Abbas, and H. F. Khazaal, "A review of non-isolated bidirectional DC-DC converters for hybrid energy storage system," in *Proc. IICETA 2022*, pp. 248–253, 2022.
10. R. Pramanik and B. B. Pati, "Modelling and control of a non-isolated half-bridge bidirectional DC-DC converter with an energy management topology applicable with

- EV/HEV,” *Journal of King Saud University – Engineering Sciences*, vol. 35, no. 2, pp. 116–122, 2023.
11. K. Varesi et al., “Performance and design analysis of an improved non-isolated multiple input buck DC–DC converter,” *IET Power Electronics*, vol. 10, no. 9, pp. 1034–1045, 2017.
 12. H. Shayeghi, S. Pourjafar, and S. M. Hashemzadeh, “A switching capacitor based multi-port bidirectional DC–DC converter,” *IET Power Electronics*, vol. 14, no. 9, pp. 1622–1636, 2021.
 13. [13] S. Punna, U. B. Manthathi, and A. C. Raveendran, “Modeling, analysis, and design of novel control scheme for two-input bidirectional DC–DC converter for HESS in DC microgrid applications,” *International Transactions on Electrical Energy Systems*, vol. 31, no. 10, e12774, 2021.
 14. Z. Saadatizadeh et al., “A new non-isolated free ripple input current bidirectional DC–DC converter with capability of zero voltage switching,” *International Journal of Circuit Theory and Applications*, vol. 46, no. 3, pp. 519–542, 2018.
 15. X. Qi, Y. Wang, Y. Wang, and Z. Chen, “Optimization of centralized equalization systems based on an integrated cascade bidirectional DC–DC converter,” *IEEE Transactions on Industrial Electronics*, vol. 69, no. 1, pp. 249–259, 2021.
 16. M. A. Khan, A. Ahmed, I. Husain, Y. Sozer, and M. Badawy, “Performance analysis of bidirectional DC–DC converters for electric vehicles,” *IEEE Transactions on Industry Applications*, vol. 51, no. 4, pp. 3442–3452, 2015.
 17. R. R. De Melo, F. L. Tofoli, S. Daher, and F. L. M. Antunes, “Interleaved bidirectional DC–DC converter for electric vehicle applications based on multiple energy storage devices,” *Electrical Engineering*, vol. 102, pp. 2011–2023, 2020.
 18. S. Bahravar, K. Abbaszadeh, and J. Olamaei, “High step-up non-isolated DC–DC converter using diode–capacitor cells,” *Iranian Journal of Science and Technology*, (incomplete details).
 19. M. P. Mohandass and S. Manoharan, “Hybrid technique Vienna rectifier based topology for FCS electric vehicle using AC–DC converter,” *Analog Integr. Circuits Signal Process.*, vol. 122, art. no. 41, Feb. 2025.
 20. R. Islam, S. M. S. H. Rafin, and O. A. Mohammed, “Comprehensive review of power electronic converters in electric vehicle applications,” *Forecasting*, vol. 5, no. 1, pp. 22–80, 2023, doi: 10.3390/forecast5010002
 21. S. K. Paramasivam, R. Senniyappan, S. K. Ramu, and S. Mani, “IIPQ controlled three-phase three-level four-wire T-type Vienna rectifier for high efficient off-board fast EV charging station with enhanced system stability,” *Results in Engineering*, 2025, doi: 10.1016/j.rineng.2025.106880
 22. M. P. Mohandass and S. Manoharan, “Hybrid technique Vienna rectifier based topology for FCS electric vehicle using AC–DC converter,” *Analog Integr. Circuits Signal Process.*, vol. 122, art. no. 41, Feb. 2025.



23. R. Islam, S. M. S. H. Rafin, and O. A. Mohammed, "Comprehensive review of power electronic converters in electric vehicle applications," *Forecasting*, vol. 5, no. 1, pp. 22–80, 2023, doi: 10.3390/forecast5010002.
24. S. K. Paramasivam, R. Senniyappan, S. K. Ramu, and S. Mani, "IIPQ controlled three-phase three-level four-wire T-type Vienna rectifier for high efficient off-board fast EV charging station with enhanced system stability," *Results in Engineering*, 2025, doi: 10.1016/j.rineng.2025.106880.
25. S. B. Kumbhar and S. Y. Gadgune, "A comprehensive review on optimization techniques of controller based Vienna rectifier used for electric vehicle charging system," in *Proc. 1st Int. Conf. Sustainability and Technological Advancements in Engineering Domain (SUSTAINED)*, Faridabad, India, Dec. 2024, doi: 10.1109/SUSTAINED63638.2024.11074097.
26. M. M. Rana, S. M. M. Alam, F. A. Rafi, S. B. Deb, B. Agili, and M. He, "Comprehensive review on the charging technologies of electric vehicles (EV) and their impact on power grid," *IEEE Access*, 2024.